Journal of Biogeography (J. Biogeogr.) (2015) 42, 315–327

ORIGINAL ARTICLE

Phylogeography and evolution of three closely related species of *Tsuga* (hemlock) from subtropical eastern Asia: further insights into speciation of conifers

Yu-Zhi Cun[1,2] and Xiao-Quan Wang[1,*]

[1]State Key Laboratory of Systematic and Evolutionary Botany, Institute of Botany, Chinese Academy of Sciences, Beijing 100093, China, [2]Dali University, Dali 671003, China

*Correspondence: Xiao-Quan Wang, State Key Laboratory of Systematic and Evolutionary Botany, Institute of Botany, Chinese Academy of Sciences, 20 Nanxincun, Xiangshan, Beijing 100093, China.
E-mail: xiaoq_wang@ibcas.ac.cn

ABSTRACT

Aim The biogeography and speciation of conifers are of special interest because of the ecological importance of these trees, but the boundaries and evolutionary relationships of closely related species of conifers are difficult to disentangle. To investigate how lineage sorting and gene flow affect species boundaries in conifers, we studied the population genetic structure and phylogeographical history of the *Tsuga chinensis–T. forrestii* complex and compared the results with those for a closely related species, *T. dumosa*.

Location Subtropical eastern Asia.

Methods Phylogeographical analyses, in combination with coalescent simulations, were performed based on sequence variation of paternal chloroplast and maternal mitochondrial DNA in 1368 individuals from 52 populations of the three *Tsuga* (hemlock) species.

Results Mitotypes were shared extensively among the three species while the chlorotypes were relatively more species-specific. Two genetic breaks and thus three distinct geographical groups were identified in the *T. chinensis–T. forrestii* species pair. Unidirectional pollen flow from *T. forrestii* to *T. chinensis* was detected.

Main conclusions *Tsuga forrestii* originated from a pre-existing isolate of *T. chinensis*, and a cryptic genetic break formed between eastern and western populations of the latter. Incomplete lineage sorting was responsible for the extensive sharing of mitotypes among the three hemlock species, and our results seem to support the idea that paternally inherited markers are more effective in delimiting species than maternally inherited markers. We also found that hemlock populations in the Himalayas were very likely to have experienced extinction, but that most populations in other areas of subtropical mainland China survived the late Quaternary glacial cycles by elevational shifts.

Keywords

Eastern Asia, gene flow, glacial refugia, incomplete lineage sorting, peripatric speciation, phylogeography, population differentiation, southern China, species delimitation, *Tsuga*.

INTRODUCTION

The sharing of allelic polymorphism as a result of interspecific gene flow (e.g. Matos & Schaal, 2000; Zhou *et al.*, 2010) or incomplete lineage sorting (e.g. Ran *et al.*, 2006; Jaramillo-Correa *et al.*, 2008) is common in conifers that are characterized by ecological and life-history traits favouring large effective population sizes, such as wind pollination, wide geographical distributions, and centuries-long fertile life spans (e.g. Willyard *et al.*, 2009). Hence, gene flow and lineage sorting affecting the species boundary and delimitation of closely related congeners of conifers are of special interest for evolutionary genetics.

Based on spatially explicit simulations, Currat *et al.* (2008) predicted that the frequency of gene introgression between species is negatively correlated with the rate of intraspecific gene flow. Du *et al.* (2009) and Petit & Excoffier (2009) further proposed that genetic markers experiencing high rates of

Journal of Biogeography

gene flow should be more effective in delimiting species than those experiencing low gene flow, given the effects of high intraspecific gene flow in preventing interspecific introgression (Currat *et al.*, 2008). In contrast, Zhou *et al.* (2010) reported that, owing to accelerated lineage sorting, the markers experiencing high intraspecific gene flow are more species-specific than those experiencing low intraspecific gene flow. In Pinaceae, the chloroplast and mitochondrial genomes show predominantly paternal and maternal inheritance, respectively (Mogensen, 1996), and the chloroplast genome experiences higher rates of gene flow than the mitochondrial genome (Petit *et al.*, 2005). Thus, by comparing sequence variation of mitochondrial DNA (mtDNA) and chloroplast DNA (cpDNA) in a group of closely related species in Pinaceae, we can directly test the hypothesis that genetic markers experiencing high rates of gene flow are more effective in differentiating species (Petit & Excoffier, 2009), and disentangle the effects of high intraspecific gene flow on preventing introgression and promoting lineage sorting.

Tsuga (hemlock), a genus of Pinaceae comprising nine to ten species, is an important constituent of subalpine forest communities in North America and East Asia (Havill *et al.*, 2008). Three species, *T. chinensis* (Franchet) Pritz., *T. forrestii* Downie and *T. dumosa* (D. Don) Eichler, occur in montane areas of subtropical eastern Asia, a region with the most diverse temperate flora in the Northern Hemisphere (Qiu *et al.*, 2011). *Tsuga chinensis* is more or less continuous in its distribution, extending broadly from the eastern Hengduan Mountains eastward to the Huang/Tianmu and Yandang/Wuyi Mountains at an elevation of 1000–2900 m above sea level (a.s.l.). In contrast, *T. forrestii* has a narrow range, restricted to the central Hengduan Mountains at approximately 2800 m a.s.l. *Tsuga dumosa* occurs in the Hengduan Mountains and the eastern Himalayas at 2000–3600 m a.s.l. Recent phylogenetic work on *Tsuga* (Havill *et al.*, 2008) suggested that *T. dumosa*–*T. chinensis*-Taiwan (*T. chinensis* from Taiwan Island) are sister to a clade comprising *T. forrestii*, *T. chinensis* (*T. chinensis* from mainland China) and *T. sieboldii* (a species endemic to Japan). *Tsuga chinensis* and *T. forrestii* were recovered as the most recently diverged species pair (Havill *et al.*, 2008). On this basis, Havill *et al.* (2008) suggested that *T. chinensis*-Taiwan should be treated as a separate species. The three hemlock species from subtropical eastern Asia are especially suitable for investigating the phylogeographical history in conifers and the factors affecting species boundaries, such as lineage sorting and gene flow, because of their phylogenetic relationships and recent divergence.

We present a phylogeographical and evolutionary study of the *T. chinensis*–*T. forrestii* species pair and compare the results with those for *T. dumosa*. Specifically, our three main objectives were: (1) to investigate the genetic structure and phylogeographical history of the *T. chinensis*–*T. forrestii* species pair and explore the origin of *T. forrestii*; (2) to test whether chlorotypes are more species-specific than mitotypes in the three hemlock species; and (3) to examine the effects of lineage sorting and gene flow on trans-species polymorphism and species delimitation. In order to address these objectives, we examined sequence variation in the mitochondrial *nad*5 intron 1 and three cpDNA fragments (*trn*S/fM, *atp*H/I and *psb*J/*pet*A) in 34 populations. In combination with sequence data from our previous work of *T. dumosa* (Cun & Wang, 2010), we used these sequences to perform comparative phylogeographical analyses.

MATERIALS AND METHODS

Population sampling

Leaf samples were collected from 34 populations representing 865 trees, including 776 trees from 31 populations of *Tsuga chinensis* and 89 trees from three populations of *T. forrestii*. Sampling covered almost the entire ranges of both species (Fig. 1, and see Appendix S1 in the Supporting Information). Each population was represented by 19–35 individuals that were at least 100 m apart, with the exception of four populations (TQ, HS, EMS and WC) where 2–5 individuals were collected. Considering that three of the four markers (*nad*5 intron 1, *trn*S/fM and *atp*H/I) were used in our previous phylogeographical work of *T. dumosa*, which represented a sampling of 503 trees from 18 populations (Cun & Wang, 2010), here we combined the mt- and cp-DNA data of this species with that of *T. chinensis*–*T. forrestii* (totalling 1368 individuals) for comparative phylogeographical analyses. Following the suggestion of Havill *et al.* (2008), *T. chinensis*-Taiwan was treated as an independent taxon, and two individuals were included in analyses. Based on the phylogeny of *Tsuga* (Havill *et al.*, 2008), we sampled 13 individuals that represent all other species of the genus (with the exception of *T. caroliniana*) and two individuals of *Nothotsuga longibracteata* as outgroups. Detailed information on samples is presented in Appendix S1.

DNA extraction, gene amplification and sequencing

DNA extraction and PCR amplification followed Cun & Wang (2010). The mtDNA *nad*5 intron 1 and three cpDNA intergenic spacers (*trn*S/fM, *atp*H/I and *psb*J/*pet*A) were amplified and directly sequenced using primers shown in Appendix S1.

Samples from all 865 individuals of *T. chinensis*–*T. forrestii*, 13 of other *Tsuga* species and two of *Nothotsuga longibracteata* were analysed with *nad*5 and the three cpDNA markers. The *psb*J/*pet*A region was sequenced for 18 individuals from 18 populations of *T. dumosa*. The sequences reported in this study are deposited in GenBank under accession numbers KF828306–KF828740.

Data analyses

Arlequin 3.11 (Excoffier *et al.*, 2005) was used to estimate molecular diversity indices, including number of segregating

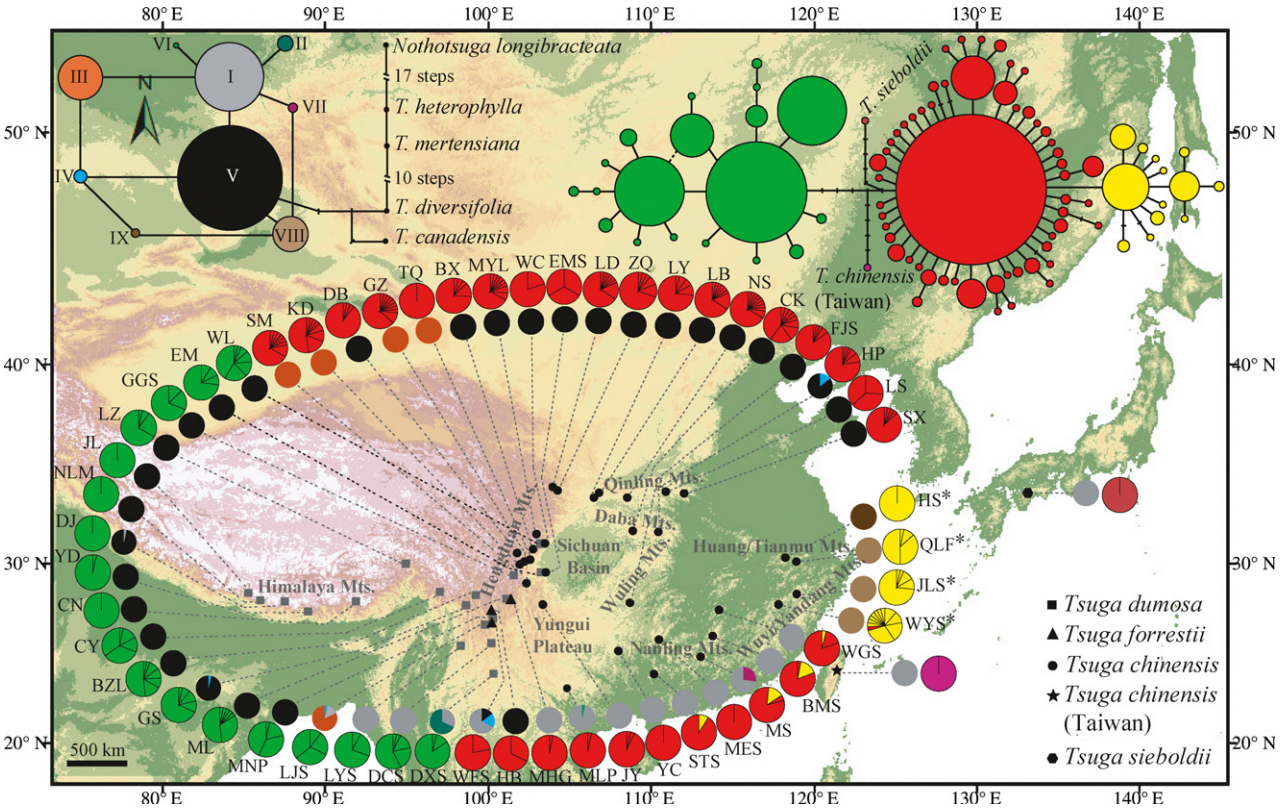

Figure 1 Geographical distributions of the clades of chlorotypes (in outer circles) and mitotypes (in inner circles) detected in the three hemlock (*Tsuga*) species from subtropical eastern Asia, with networks of the mitotypes (upper left) and chlorotypes (upper right) constructed with TCS 1.21. The chlorotypes were designated based on *trn*S/fM and *atp*H/I. The sizes of the circles in the network are proportional to the observed frequencies of the haplotypes. Each section of the circle represents one haplotype. More information on the populations is given in Appendix S1. *Tsuga chinensis* comprises 31 populations that were divided into two geographical groups: western *T. chinensis* and eastern *T. chinensis* (*).

sites (S), number of haplotypes (H), haplotype diversity (H_d) and nucleotide diversity (π). The haplotype richness (A) was calculated by dividing the number of haplotypes by the sample size.

TCS 1.21 was used to construct haplotype networks (Clement *et al.*, 2000). The ambiguities in the cpDNA network were refined following Crandall & Templeton (1993). PERMUT (Pons & Petit, 1996) was used to calculate average population genetic diversity (H_S), total genetic diversity (H_T), and population differentiation values (G_{ST}, N_{ST}). The four measures were estimated for all three hemlock species based on mtDNA, but were calculated only for *T. chinensis*–*T. forrestii* and different geographical groups of *T. chinensis* using cpDNA.

A spatial analysis of molecular variance (SAMOVA) was performed with cpDNA to identify groups of populations that are geographically homogenous in *T. chinensis*–*T. forrestii*, using SAMOVA 1.0 (Dupanloup *et al.*, 2002). This program iteratively seeks the composition of a user-defined number (K) of groups of geographically adjacent populations that maximizes F_{CT}, i.e. the proportion of genetic variation among groups.

Analyses of molecular variance (AMOVAs; Excoffier *et al.*, 1992) were conducted to partition genetic variation among geographical groups, among populations within geographical groups and within populations for all three hemlock species based on mtDNA, but only for *T. chinensis*–*T. forrestii* and different geographical groups of *T. chinensis* using cpDNA. Significance was tested using a nonparametric permutation procedure with 1000 permutations. Population expansion events were detected by Fu's F_S neutrality test (Fu, 1997). The *P*-values were generated using 1000 simulations under a model of selective neutrality. All analyses were performed with ARLEQUIN 3.11.

The isolation-with-migration (IM) model offers an analytical framework that can distinguish between incomplete lineage sorting and interspecific gene flow as explanations for observed patterns of genetic divergence (Nielsen & Wakeley, 2001). Using the program IMA (Hey & Nielsen, 2007), we applied the IM model to the sequence data from three cpDNA loci (*trn*S/fM, *atp*H/I and *psb*J/*pet*A) for two divergence events: (1) *T. forrestii*–western *T. chinensis*; and (2) western *T. chinensis*–eastern *T. chinensis* (referring to the geographical groups identified by the SAMOVA analysis). Analyses in IMA were run under the Hasegawa–Kishino–Yano (HKY) mutation model (Hasegawa *et al.*, 1985). The mutation scalar of cpDNA was set to 0.5, as the effective population size of the chloroplast genome is one-half that of

the nuclear genome for a monoecious plant (Birky *et al.*, 1983). Further, because IMa cannot accommodate gaps or missing data in DNA alignments, indels were removed.

By applying the Markov chain Monte Carlo method, IMa yielded the estimates of six demographic parameters scaled by mutation rate, including population-split time (t), effective population sizes for the ancestral and two descendant populations (θ_A, θ_1, θ_2), and migration rates between the descendant populations (m_1, m_2). The posterior probability densities of the model parameters were generated by simulating a Markov chain having a stationary distribution proportional to that of density. The IMa simulation was set to a 500,000 burn-in period to make the chain independent of the starting state and continued for 80 million simulations. The peaks of resulting distributions were interpreted as the maximum likelihood estimates (MLEs) of the parameters with credibility intervals equalling the 90% highest posterior density (HPD) intervals. Three independent runs with different seed numbers were performed to ensure convergence, and the lowest effective sample size (ESS) among the six parameters was at least 50 in each run, as recommended in IMa. Upper bounds for the prior distributions of the parameters were set empirically after preliminary runs with larger parameter intervals. To convert the MLEs and 90% HPD intervals for population-split time (t) to time in years since divergence (T), $T = t/\mu$ was taken. The mutation rate (μ) was estimated using BEAST 1.7.5 (see Appendix S2). Two methods were tried to calibrate the molecular clock: (1) only the most recent common ancestor of *Tsuga* and *Nothotsuga* was fixed at an age of 90 Ma based on the oldest pollen record of *Tsuga* from the Late Cretaceous deposits in Poland (reviewed in Havill *et al.*, 2008); and (2) another calibration was added, and the crown age of *Tsuga* was set with a normal prior distribution of 47 $\pm$ 4.9 Ma, based on the earliest record of *Tsuga* megafossils from the Eocene deposits (Appendix S2), which is consistent with the crown age of *Tsuga* estimated by Havill *et al.* (2008).

RESULTS

Chloroplast DNA variation

A total of 87 chlorotypes were identified based on sequence variation of *trn*S/fM and *atp*H/I in 1368 trees from 52 populations of the three hemlock species (see Appendix S3). Nineteen chlorotypes from 503 individuals of *Tsuga dumosa* (indicated in green) and 68 chlorotypes from 865 individuals of *T. chinensis–T. forrestii* (indicated in red and yellow) formed two distinct clades with six mutations separating them (Fig. 1). When *psb*J/*pet*A sequences were added, 132 chlorotypes were identified from 865 individuals of *T. chinensis–T. forrestii* (Fig. 2, Appendix S3).

Based on cpDNA of *T. chinensis–T. forrestii*, the SAMOVA tests (K = 2–33) indicated that the F_{CT} value reached a plateau at $K = 3$. For $K \geq 4$, at least one of the groups contained a single population. We retained the configuration of $K = 3$ ($F_{CT} = 0.429$, $F_{SC} = 0.115$, $P < 0.001$ for both) and found that the composition of groups corresponded strongly to the geographical distribution of chlorotypes (Fig. 2). Two phylogeographical breaks and three distinct geographical groups were identified in the range of *T. chinensis–T. forrestii*. Group 1 (*T. forrestii*) comprised all three *T. forrestii* populations; Group 2 (eastern *T. chinensis*) consisted of four *T. chinensis* populations in East China (HS, QLF, JLS and WYS); and Group 3 (western *T. chinensis*) included the remaining 27 *T. chinensis* populations (Fig. 2, Appendix S3).

In the network of cpDNA haplotypes, many derived haplotypes showed a satellite-like distribution (Fig. 2), and the network direction was inferred based on the phylogenetic reconstruction of *Tsuga* species (Appendix S2). *Tsuga forrestii* had only the six chlorotypes of clade c2 (c2 and its derived haplotypes) and genetic diversity was relatively low ($A = 0.067$, $\pi = 0.00036$, $H_d = 0.663$, Table 1; $H_S = 0.632$, $H_T = 0.678$, Table 2). Eastern *T. chinensis* possessed the 18 chlorotypes of clade c120 (c120 and its derived haplotypes), except one individual from population WYS which exhibited haplotype c16 (Fig. 2, Appendix S3), and genetic diversity was high ($A = 0.213$, $\pi = 0.00091$, $H_d = 0.790$, Table 1; $H_S = 0.771$, $H_T = 0.819$, Table 2). Western *T. chinensis* contained the remaining haplotype clades, except that 16 individuals from four populations (JY, KD, GZ and DB) geographically adjacent to *T. forrestii* possessed three haplotypes of clade c2, and 10 individuals from four populations (WGS, BMS, MS and STS) exhibited haplotype c106 of clade c120 (Fig. 2). In total, western *T. chinensis* had 112 haplotypes (Appendix S3), showing very high genetic diversity ($A = 0.163$, $\pi = 0.00077$, $H_d = 0.883$, Table 1; $H_S = 0.828$, $H_T = 0.930$, Table 2). Of the 132 chlorotypes in *T. chinensis–T. forrestii*, 44 were shared among populations, but only 11 of them had a frequency higher than 2%. Up to 88 chlorotypes were specific to 26 populations (Fig. 2, Appendix S3). When populations EMS, TQ, WC and HS were excluded from the analysis because of small sample size, nearly all *T. chinensis* populations possessed private haplotypes. The Fu's F_S test showed significantly negative values for the species pair, western and eastern *T. chinensis*, and about half of the populations had an excess of rare haplotypes over what would be expected under neutrality (Table 1). The levels of genetic differentiation were moderate for *T. forrestii*, western and eastern *T. chinensis* ($G_{ST} = 0.068$, 0.110 and 0.059, respectively). A significant phylogeographical structure was detected in *T. forrestii*, *T. chinensis*, and the species pair ($N_{ST} > G_{ST}$, $P < 0.05$ for all; Table 2).

Mitochondrial DNA variation

For the 1368 individuals of the three hemlock species, *nad*5 intron 1 had five variable sites, which were used to designate nine distinct mitotypes. Five, eight and three mitotypes were detected in *Tsuga dumosa*, *T. chinensis* and *T. forrestii*, respectively (Fig. 1, Appendix S3). Four mitotypes were shared among species, including mitotype III between *T.*

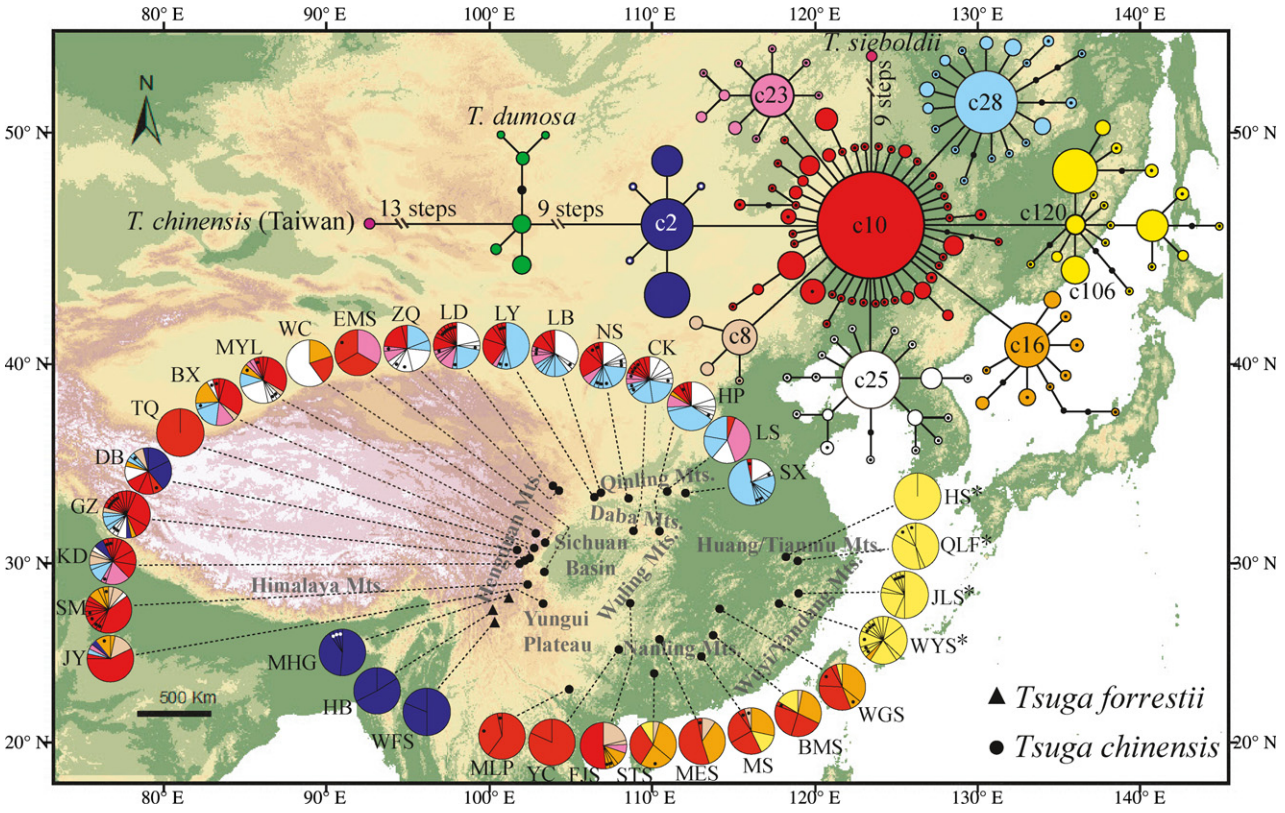

Figure 2 Geographical distributions in subtropical eastern Asia of the clades of chlorotypes detected in populations of the *Tsuga chinensis–T. forrestii* species pair, with the network of chlorotypes (upper right) constructed by TCS 1.21. The chlorotypes were designated based on sequence variation in *trn*S/fM, *atp*H/I and *psb*J/*pet*A. The sizes of the circles in the network are proportional to the observed frequencies of the haplotypes. Each section of the circle represents one haplotype, and the sections containing a point represent population-specific haplotypes. *Tsuga chinensis* comprises 31 populations that were divided into two geographical groups: western *T. chinensis* and eastern *T. chinensis* (*).

dumosa and *T. chinensis*, and mitotypes I, IV and V among all three species. Mitotype V (frequency: 56.7%) occurred from the Himalayas through the central and eastern Hengduan Mountains to the Qingling-Daba Mountains in Central China, while mitotype I (16.0%) extended from the Himalayas through the central and southern Hengduan Mountains and the northern Yungui Plateau to the Nanling Mountains in South China. In contrast, the remaining five species-specific mitotypes had a restricted peripheral distribution. For instance, mitotypes II and VI occurred in the southernmost populations of *T. dumosa* and *T. chinensis*, respectively, and VIII in three populations of *T. chinensis* in East China.

Only eight of the 52 surveyed populations were polymorphic (Fig. 1, Appendix S3). Genetic differentiation across the entire geographical range of all three hemlock species was high (G_{ST} = 0.928, N_{ST} = 0.940), with a significant phylogeographical structure ($N_{ST} > G_{ST}$, $P < 0.05$; Table 2). Moreover, the AMOVA analysis showed that the difference between *T. dumosa* and *T. chinensis–T. forrestii* explained less than 5.0% of the total mtDNA variation, while most of the variance (94.3%) existed among populations (Table 2). When the *T. chinensis–T. forrestii* species pair was considered separately, 40.3% of the variation occurred among the three geographical groups (*T. forrestii*, western *T. chinensis* and eastern *T. chinensis*).

IM analysis

Three independent runs of IMa yielded unambiguous marginal posterior probability distributions of the parameters for two pairwise analyses (Fig. 3). The MLEs and 90% HPD intervals of one simulation are shown in Table 3. The substitution rate of the combined *trn*S/fM + *atp*H/I + *psb*J/*pet*A sequences (μ) was consistently estimated to be 0.57×10^{-6} per year based on its length used for the pairwise analyses (2040 bp for *T. forrestii*–western *T. chinensis* and 2029 bp for western *T. chinensis*–eastern *T. chinensis* after excluding indels), and its mutation rate (per site per year) was estimated to be 0.28×10^{-9} by using one calibration and 0.20×10^{-9} by using two calibrations (Appendix S2). We also tried to set different prior values for the second calibration point (the crown age of *Tsuga*), and found that the divergence time estimates were sensitive to the prior. Therefore, the mutation rate 0.28×10^{-9} based on one calibration was used in the IM analysis.

Tsuga forrestii versus western *T. chinensis*: the MLEs of effective population size (θ, scaled by mutation rate) for *T.*

Table 1 Genetic parameters and results of Fu's F_S tests of 34 populations of the *Tsuga forrestii–T. chinensis* species pair from subtropical eastern Asia. See Appendix S1 for locational details of each population.

			mtDNA			cpDNA						
Species	Pop	*n*	*S*	*H*	*ph*	*S*	*H*	*ph*	*A*	π	H_d	F_S
Tsuga forrestii	WFS	27	2	3	0	2	3	0	0.111	0.00037	0.672	1.148
	HB	31	0	1	0	2	3	0	0.097	0.00032	0.624	0.885
	MHG	31	0	1	0	4	5	3	0.161	0.00031	0.600	−1.501
	total	89	2	3	0	5	6	3	0.067	0.00036	0.663	−1.042
Western *Tsuga chinensis*†	SM	27	0	1	0	21	14	5	0.519	0.00095	0.835	−8.333***
	EMS	3	0	1	0	3	3	1	–‡	–	–	–
	TQ	2	0	1	0	0	1	0	–	–	–	–
	WC	5	0	1	0	3	3	0	–	–	–	–
	GZ	30	0	1	0	23	19	6	0.633	0.00104	0.924	−16.018***
	KD	29	0	1	0	14	15	6	0.517	0.00098	0.941	−9.285***
	DB	28	0	1	0	12	11	2	0.393	0.00086	0.905	−4.555**
	BX	23	0	1	0	12	9	3	0.391	0.00082	0.858	−3.110*
	MYL	30	0	1	0	15	13	4	0.433	0.00076	0.860	−7.840**
	ZQ	26	0	1	0	11	10	3	0.385	0.00092	0.892	−3.282*
	LD	32	0	1	0	19	16	8	0.500	0.00096	0.903	−10.336***
	LY	30	0	1	0	10	9	4	0.300	0.00061	0.747	−3.649*
	LB	30	0	1	0	12	14	3	0.467	0.00084	0.876	−8.704***
	NS	30	0	1	0	15	14	7	0.467	0.00086	0.915	−8.521***
	LS	19	0	1	0	4	5	0	0.263	0.00073	0.784	0.165
	SX	30	0	1	0	10	9	4	0.300	0.00055	0.722	−4.156**
	CK	25	0	1	0	16	13	7	0.520	0.00107	0.940	−11.599***
	HP	35	1	2	0	12	13	2	0.371	0.00073	0.825	−7.367***
	FJS	33	0	1	0	7	8	2	0.242	0.00045	0.695	−3.573**
	JY	27	0	1	0	7	8	1	0.296	0.00044	0.675	−4.100**
	BMS	31	0	1	0	6	6	1	0.194	0.00065	0.796	−0.392
	WGS	25	0	1	0	6	6	2	0.240	0.00051	0.763	−1.395
	MES	31	0	1	0	3	4	1	0.129	0.00031	0.617	−0.356
	STS	22	0	1	0	5	5	1	0.227	0.00057	0.771	−0.270
	YC	33	0	1	0	1	2	0	0.061	0.00013	0.307	0.811
	MLP	30	1	2	0	2	3	2	0.100	0.00024	0.513	0.243
	MS	21	1	2	0	7	6	2	0.286	0.00069	0.819	−0.793
	total	687	4	6	2	98	112	107	0.163	0.00077	0.883	−26.836***
Eastern *Tsuga chinensis*†	WYS	27	0	0	0	18	14	6	0.519	0.00116	0.912	−6.814***
	JLS	30	0	0	0	8	8	3	0.267	0.00068	0.715	−2.154
	QLF	30	0	0	0	7	5	2	0.167	0.00087	0.685	1.365
	HS	2	0	0	1	0	1	0	–	–	–	–
	total	89	1	2	2	23	19	17	0.213	0.00091	0.790	−9.007**
T. chinensis	total	776	3	8	3	115	129	85	0.166	0.00091	0.905	−26.389***
Species pair	total	865	4	8	3	117	132	88	0.153	0.00094	0.919	−26.262***

The parameters include sample size (*n*), number of segregating sites (*S*), number of haplotypes (*H*), number of private haplotypes (*ph*), haplotype richness (*A*), nucleotide diversity (π), and haplotype diversity (H_d). The latter three parameters and F_S were not calculated for mtDNA because of low variation.

†*Tsuga chinensis* in two geographical regions; ‡Populations EMS, TQ, WC and HS were excluded from the analysis because of small sample size; *$0.05 > P \geq 0.01$; **$0.01 > P \geq 0.001$; ***$P < 0.001$.

forrestii, western *T. chinensis*, and their ancestral population were 0.464 (90% HPD: 0.127–1.308), 113.889 (68.333–194.877), and 2.911 (0.886–7.213), respectively (Fig. 3a–c). The migration parameter of the direction from western *T. chinensis* to *T. forrestii* (m_1) had a peak at zero, indicating that no gene flow had occurred, while that from *T. forrestii* to western *T. chinensis* (m_2) showed a peak at 0.265 (90% HPD: 0.095–0.673) (Fig. 3d–e). The marginal posterior probability of the divergence time parameter (*t*) revealed a sharp peak at 0.213, with a narrow distribution (Fig. 3f). When converted to a scale in years, the divergence time between *T. forrestii* and western *T. chinensis* was estimated to be 0.374 Ma (90% HPD: 0.256–0.539 Ma).

Eastern *T. chinensis* versus western *T. chinensis*: the MLEs of effective population sizes for eastern *T. chinensis*, western *T. chinensis*, and their ancestral population were 3.173 (90% HPD: 1.503–6.847), 77.534 (40.318–139.561), and 2.362 (0.262–7.085), respectively (Fig. 3g–i). The migration parameter of the direction from western *T. chinensis* to eastern *T. chinensis* (m_1) showed a peak at 0.126 (90% HPD:

Table 2 Estimates of population genetic diversity and differentiation (mean ± SE in parentheses) using PERMUT and analysis of molecular variance (AMOVA) based on mitotypes and chlorotypes detected in three *Tsuga* species from subtropical eastern Asia.

Species or population groups		PERMUT				AMOVA
		H_S	H_T	G_{ST}	N_{ST}	$F_{ST}(F_{CT})$
Mitotype	*T. dumosa*	0.050 (0.0296)	0.398 (0.1353)	0.873 (0.0524)	0.906 (0.025)§	0.907***
	T. forrestii	0.173 (0.1728)	0.728 (0.1019)	0.763 (0.3153)	0.673 (0.4074)	0.703***
	T. chinensis	0.026 (0.0169)	0.695 (0.0562)	0.963 (0.0242)	0.973 (0.0179)§	0.972***
	T. chinensis–T. forrestii†	0.040 (0.0218)	0.691 (0.0509)	0.943 (0.031)	0.949 (0.031)§	0.962*** (0.403***)
	T. dumosa + *T. chinensis–T. forrestii*‡	0.043 (0.0174)	0.607 (0.059)	0.928 (0.027)	0.940 (0.025)§	0.943*** (0.050^{NS})
Chlorotype	*T. forrestii*	0.632 (0.0213)	0.678 (0.0093)	0.068 (0.063)	0.112 (0.102)§	0.118***
	T. chinensis	0.789 (0.0269)	0.917 (0.0169)	0.140 (0.0223)	0.223 (0.0437)§	0.233***
	western *T. chinensis*	0.828 (0.0274)	0.930 (0.0162)	0.110 (0.018)	0.219 (0.005)§	0.121***
	eastern *T. chinensis*	0.771 (0.0711)	0.819 (0.0658)	0.059 (0.03)	0.042 (NC)	0.039^{NS}
	T. chinensis–T. forrestii†	0.774 (0.0257)	0.929 (0.0144)	0.166 (0.025)	0.289 (0.049)§	0.495*** (0.429***)

†All 34 populations of the *T. chinensis–T. forrestii* species pair were divided into three geographical groups (*T. forrestii*, western *T. chinensis* and eastern *T. chinensis*).

‡All 52 populations of *T. dumosa*, *T. chinensis* and *T. forrestii* were divided into two groups (*T. dumosa*, and the *T. chinensis–T. forrestii* species pair).

The parameters include average population genetic diversity (H_S), total genetic diversity (H_T), population differentiation values (G_{ST}, N_{ST}), proportion of genetic variation among populations (F_{ST}), and proportion of genetic variation among population groups (F_{CT}). Significance testing (1000 permutations): $^{\S}N_{ST}$ is significantly higher than G_{ST} ($0.01 < P < 0.05$); $^{NS}P \geq 0.05$; $*0.05 > P \geq 0.01$; $***P < 0.001$.

Table 3 Maximum-likelihood estimates (MLEs) and the 90% highest posterior density (HPD) intervals of demographic parameters for the *Tsuga chinensis–T. forrestii* species pair from subtropical eastern Asia.

Comparison	Estimates	θ_1	θ_2	θ_A	m_1	m_2	t	T (Ma)
T. forrestii vs. western *T. chinensis*	MLE	0.464	113.889	2.911	0.005	0.265	0.213	0.374
	$HPD90_{Lo}$	0.127	68.333	0.886	0.005	0.095	0.146	0.256
	$HPD90_{Hi}$	1. 308	194.877	7.213	2.925	0.673	0.307	0.539
eastern *T. chinensis* vs. western *T. chinensis*	MLE	3.173	77.534	2.362	0.126	0.003	0.389	0.682
	$HPD90_{Lo}$	1.503	40.318	0.262	0.002	0.001	0.223	0.391
	$HPD90_{Hi}$	6.847	139.561	7. 085	0.946	0.064	0.779	1.367

The MLEs are the locations of the peaks in the curves shown in Fig. 3.

The 90% HPD intervals are the shortest spans, along the *x* axes of Fig. 3, that contain 90% of the area of those histograms.

The parameters include effective population sizes of two descendant populations (θ_1, θ_2) and their ancestral population (θ_A), migration rates between the descendant populations (m_1, m_2), population-split time scaled by mutation rate (t), and population-split time in years (T).

0.002–0.946) (Fig. 3j), while that from eastern *T. chinensis* to western *T. chinensis* (m_2) had a peak approaching zero (Fig. 3k). The marginal posterior probability of the splitting time showed a sharp peak at 0.389, with a narrow distribution (Fig. 3l). When converted to a scale in years, the divergence time between western *T. chinensis* and eastern *T. chinensis* was estimated to be 0.682 Ma (90% HPD: 0.391–1.367 Ma).

DISCUSSION

Evolution of the *Tsuga chinensis–T. forrestii* species pair

Peripatric speciation of Tsuga forrestii

To provide more evidence for the evolutionary history of the *T. forrestii–T. chinensis* species pair, our study tried the pairwise IM analysis to estimate the demographic parameters of *T. forrestii*, eastern and western *T. chinensis*, although this analysis might have some shortcomings. For *T. chinensis–T. forrestii*, several assumptions of the IM model, such as no population structure and no gene flow from unsampled populations, are violated. However, as suggested by the simulation results of Strasburg & Rieseberg (2010), the moderate levels of population structure and migration rates among the three geographical groups (*T. forrestii*, western *T. chinensis* and eastern *T. chinensis*) were unlikely to have introduced substantial bias in the parameter estimates. Additionally, we conducted a multipopulation IM analysis on the three geographical groups. Unfortunately, the results indicated that the present data may have not enough signal for estimating all parameters. Nevertheless, in the case of chimpanzees, the results of multiple two-population analyses are largely consistent with those of the full multipopulation analysis (Hey, 2010).

Because it is difficult to resolve the phylogenetic positions of *Tsuga* megafossils, we tried two methods to calibrate the

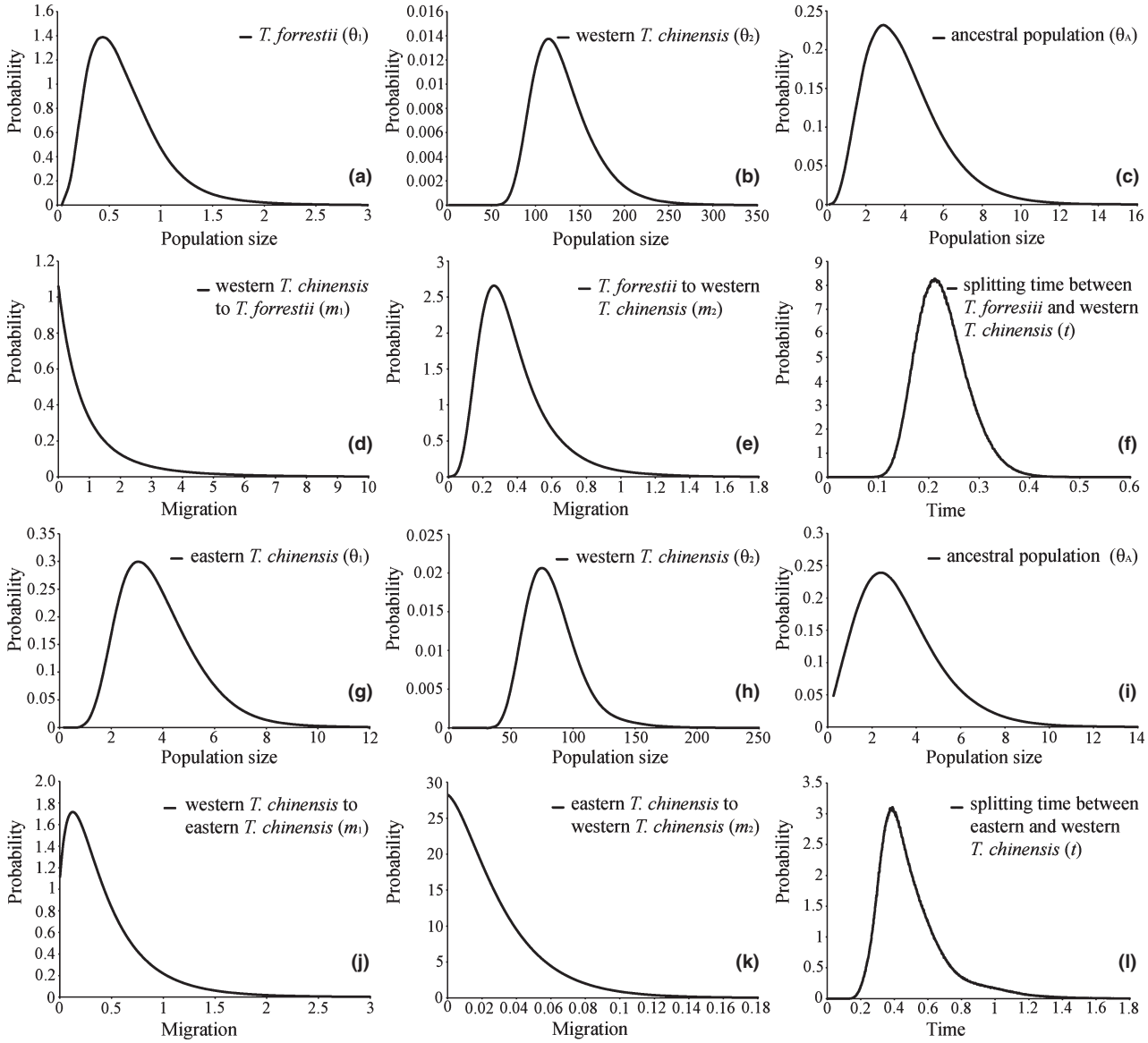

Figure 3 The marginal posterior probability distributions for various demographical parameters (scaled by the neutral mutation rate) estimated with IMA for the *Tsuga chinensis–T. forrestii* species pair from subtropical eastern Asia: (a)–(f) *T. forrestii* versus western *T. chinensis*; and (g)–(l) eastern *T. chinensis* versus western *T. chinensis*.

molecular clock. Although the substitution rate (per site per year) of the *T. chinensis–T. forrestii* lineage was estimated to be 0.28×10^{-9} (95% HPD interval: 0.07–0.42×10^{-9}) based on one calibration and 0.20×10^{-9} (95% HPD interval: 0.05–0.41×10^{-9}) based on two calibrations, the two estimates are close (Appendix S2). Therefore, while the divergence time estimates based on this substitution rate (0.28×10^{-9}) need to be used cautiously, they should not greatly affect the related inferences below.

Evidence for a progenitor-derivative species pair that originated from peripatric speciation includes a high genetic similarity between the two species, a narrower and ecologically more restricted distribution, and a lower genetic diversity for the putative derivative species relative to its progenitor. Usually, the two species can interbreed, and the genetic diversity of the derivative is generally a subset of that detected in the progenitor (Gottlieb *et al.*, 1985; Jaramillo-Correa & Bousquet, 2003). Over time, mutation and lineage sorting will lead to reciprocal monophyly (Rieseberg & Brouillet, 1994).

Tsuga forrestii is very similar to *T. chinensis*, but the later shows a considerably higher degree of morphological variation (Fu *et al.*, 1999). *Tsuga forrestii* is narrowly restricted to the central Hengduan Mountains, located to the south-west of the widespread *T. chinensis* (Zheng & Fu, 1978). Our present study further indicates that the two species are more closely related to each other than to any other species (Figs 1 & 2, Appendix S2). The split between them occurred as recently as the Pleistocene (about 0.374 Ma), and even later than the subdivision between eastern and western *T. chinensis* (about 0.682 Ma) (Table 3). In addition, we found that *T. forrestii*

is genetically depauperate compared to *T. chinensis*. Only six chlorotypes linked to a single haplotype clade were detected in *T. forrestii*, while 129 were observed in *T. chinensis* (Fig. 2, Appendix S3). The cpDNA diversity of *T. forrestii* is significantly lower than that of *T. chinensis* (Table 1). Also, *T. chinensis* had eight mitotypes, while *T. forrestii* had only three mitotypes and all were shared with the former (Fig. 1). Moreover, *T. forrestii* showed a lower frequency of private chlorotypes (3/89) than *T. chinensis* (85/776) (Fig. 2). Based on its geographical distribution, morphological similarity, and molecular evidence, *T. forrestii* is likely to have originated from a pre-existing isolate of *T. chinensis* and a likely biogeographical scenario for its origin could be inferred as follows. Climatic fluctuations and/or orogenic movements during the Qinghai-Tibetan Plateau uplift in the Pleistocene (Shi *et al.*, 1998) could drive population fragmentation, resulting in the ancestral population of *T. chinensis* becoming unequally divided. Subsequently, geographically isolated populations diverged genetically over time, and the peripheral isolate in the south-west evolved into *T. forrestii*. Genetic drift probably played a key role in the speciation process, given the small historical population size of *T. forrestii* estimated by IMa (Table 3). Importantly, based on the distribution pattern of mitotypes (Fig. 1), a vicariance event followed by complete lineage sorting of the chloroplast genome is a concise explanation for the origin of *T. forrestii*, although introgression by seed colonization events cannot be completely ruled out.

Another well-supported progenitor-derivative species pair in Pinaceae is *Picea mariana–Picea rubens*. The narrowly distributed *P. rubens* originated from transcontinentally distributed *P. mariana* during the Pleistocene (Perron *et al.*, 2000; Jaramillo-Correa & Bousquet, 2003). Peripheral isolation and rapid speciation observed in the two species pairs *Picea mariana–P. rubens* and *Tsuga chinensis–T. forrestii* are valuable for understanding the biogeography and evolution of conifers characterized by an outcrossing mating system and high gene flow among populations.

Secondary pollen flow cross the species boundary

In four *T. chinensis* populations (JY, KD, GZ and DB) geographically adjacent to *T. forrestii*, 16 individuals had three chlorotypes of clade c2 that are typical of *T. forrestii* (Fig. 2, Appendix S3). The IMa analysis based on cpDNA showed unidirectional pollen flow from *T. forrestii* to *T. chinensis* (Table 3, Fig. 3d–e), implying that interspecific gene flow is more suitable than incomplete lineage sorting for explaining the shared chlorotypes between the two species. Thus, we propose that: (1) the chlorotypes of clade c2 have been 'sorted' and fixed in *T. forrestii*; (2) mating barriers between *T. forrestii* and *T. chinensis* are not complete; and (3) secondary pollen flow occurred from *T. forrestii* to *T. chinensis*. The range shifts driven by the climatic fluctuations during the Pleistocene glacial/interglacial cycles, as inferred from the fossil record of *Tsuga* in the Hengduan Mountains (Cun & Wang, 2010), may have led to secondary contact between *T. forrestii* and *T. chinensis*. Additionally, the prevailing winds (including the southern branch of the westerly jet in the winter half year and the South Asian summer monsoon in the summer half year), which blow from south-west to north-east in the Hengduan Mountains (Yie & Gao, 1979), could potentially promote the unidirectional gene flow from *T. forrestii* to *T. chinensis*, given the timing of pollen release for these two species (Fu *et al.*, 1999).

Interspecific hybridization and introgression are common in conifers, but generally restricted to a narrow contact zone (e.g. Matos & Schaal, 2000; Poudel *et al.*, 2012). Similarly, narrow suture zones containing divergent cpDNA lineages often form after secondary contact of refugial lineages (Liepelt *et al.*, 2009; Gömöry *et al.*, 2012).

Cryptic genetic break between eastern and western T. chinensis

Based on the distribution of cpDNA variation, *T. chinensis* populations can be divided into two geographical groups. Eastern *T. chinensis* consists only of populations in the Huang/Tianmu and Yandang/Wuyi Mountains in East China, while western *T. chinensis* includes the remaining populations in south-western, central and southern China (Fig. 2, Appendix S3). With the exception of one tree from the southernmost population WYS, all samples of eastern *T. chinensis* are characterized by the chlorotypes in clade c120 (Fig. 2). In addition, eastern *T. chinensis* had two specific mitotypes VIII and IX (Fig. 1). By comparison, similar genetic discontinuity was previously detected in *Ginkgo biloba* (Gong *et al.*, 2008) and *Taxus wallichiana* var. *mairei* (Zhang *et al.*, 2009). This clear genetic break probably suggests a vicariance event that occurred between eastern and western *T. chinensis* during the Pleistocene (about 0.682 Ma) (Table 3). Moreover, the lack of pollen flow from eastern to western *T. chinensis* as estimated by IMa suggests that the sharing of chlorotype c106 between them could be attributed to incomplete lineage sorting (Fig. 2).

CpDNA is more suitable for species identification than mtDNA in Pinaceae

The chlorotypes of *Tsuga dumosa* and those of *T. chinensis–T. forrestii* form two distinct clades in the networks based on two (Fig. 1) or three cpDNA fragments (Fig. 2). *Tsuga chinensis* and *T. forrestii* also have distinct chlorotype clades, only with limited introgression (Fig. 2). In contrast, the mitotypes are shared extensively among the three hemlock species. Thus, our results support the finding that paternally inherited cpDNA markers are more effective for species delimitation than maternally inherited mtDNA markers in conifers (Du *et al.*, 2009; Petit & Excoffier, 2009).

Chlorotypes are more species-specific than mitotypes for all species complexes that have been investigated using both mtDNA and cpDNA in Pinaceae (reviewed by Du *et al.*,

2009, 2011; Zhou *et al.*, 2010). It is still controversial, however, as to why cpDNA is more suitable for species identification than mtDNA in Pinaceae. Du *et al.* (2009) hypothesized that high intraspecific gene flow of cpDNA could prevent interspecific introgression in the *Picea asperata* complex. In contrast, Zhou *et al.* (2010) proposed that high intraspecific gene flow could promote cpDNA lineage sorting in *Pinus massoniana* and *Pinus hwangshanensis*.

The extensive sharing of mitotypes among the three hemlock species is most likely to be caused by incomplete lineage sorting, given the lower levels of gene flow by seeds than by pollen. It is unlikely that *T. dumosa* exchanged genes with *T. chinensis–T. forrestii* in recent history for the following reasons. First, *T. dumosa* and *T. chinensis–T. forrestii* have been shown to have distinct chlorotype clades. Second, although *T. dumosa* occurs along with *T. forrestii* or *T. chinensis* in some mountain ranges in the central or eastern Hengduan Mountains, they maintain morphological distinctness, cpDNA integrity, and elevational separation (Fig. 1). For example, populations of *T. dumosa* and *T. forrestii* were found on the same mountain in Muli County, south-west Sichuan Province. *Tsuga dumosa*, restricted to high elevations, had mitotype V, while *T. forrestii*, found at lower elevations, had mitotype I. Additionally, the two species are easily distinguished from one another based on morphological features of leaf and cone (Cun & Wang, 2010). Third, an important signature of introgression is the sympatric sharing of geographically localized haplotypes between otherwise genetically and morphologically divergent species (e.g. Matos & Schaal, 2000; Palme *et al.*, 2004). Although mtDNA variation of the three hemlock species showed a striking pattern of phylogeographical structure that is largely species-independent, the shared mtDNA haplotypes are widespread, with no bias to sympatric or allopatric populations (Table 2, Fig. 1). In particular, the rare haplotype IV is shared among all three species, and is detected not only in three populations in the central Hengduan Mountains (LJS, GS and WFS), but also in one remote population in the Daba Mountains (HP).

Alternatively, the timing for complete lineage sorting is dependent on effective population size of the entire population. However, even if the census size of a population might remain relatively stable, its effective population size can be increased by population structure, and the increase is inversely proportional to the migration rate among demes (Nei & Takahata, 1993; Wakeley, 2000). Hence, compared to cpDNA, the low rate of mtDNA gene flow will maintain large genetic differentiation among populations in conifers (Petit *et al.*, 2005), and consequently could delay the attainment of reciprocal monophyly among species (Hoelzer, 1997; Wakeley, 2000). For instance, in *Picea*, which originated in the Early Cretaceous (Wang *et al.*, 2000; Klymiuk & Stockey, 2012), the ancestral mtDNA polymorphism is shared by the basal-most species and recently derived species (Ran *et al.*, 2006), although the extant species could be much younger than the ancient fossil species. In addition, the retained ancestral mtDNA haplotypes in Mesoamerican *Abies* can also be dated to the middle Pliocene (about 5 Ma) (Jaramillo-Correa *et al.*, 2008).

Lineage sorting of ancestral polymorphisms of mtDNA (*nad*5 intron 1) has not completed in the three hemlock species following a divergence in the Miocene (Appendix S2), but haplotypes of cpDNA (*trn*S/fM, *atp*H/I and *psb*J/*pet*A) have reached monophyly in *T. forrestii* since a separation in the Pleistocene (Table 3, Fig. 2). Therefore, it is clear that chlorotypes experiencing high intraspecific gene flow need less time to reach monophyly and are thus more suitable for species delimitation in the three hemlock species.

Different responses of the three hemlock species to the late Quaternary glaciations

Tsuga chinensis populations could have survived *in situ* by elevational shifts during the late Quaternary glaciations, at least in the Last Glacial Maximum (LGM). This scenario is supported by multiple lines of evidence including: (1) high cpDNA genetic diversity within species and populations (Table 1, Fig. 2); (2) the presence of an ancestral chlorotype (c10) throughout western *T. chinensis*; (3) the high frequencies of private chlorotypes observed in most populations; and (4) the relatively few 'missing' ancestral haplotypes in the cpDNA network (Fig. 2).

Given that the estimated population sizes of eastern *T. chinensis* and western *T. chinensis* are larger than their respective ancestral populations (Table 3), they could have undergone population growth following their split. The Fu's F_S test also indicated that over half of *T. chinensis* populations experienced population growth. Based on the distribution patterns of genetic diversity and private haplotypes (Table 1, Fig. 2), we suggest that many forest stands of *T. chinensis* experienced interglacial or post-glacial localized growth, particularly in the Hengduan Mountains and the Qinling/Daba Mountains.

The majority of phylogeographical investigations of temperate plants in Central and South China (reviewed by Qiu *et al.*, 2011; Li *et al.*, 2012) showed a similar demographic history characterized by survival in multiple localized refugia within the present distribution range, and limited recent expansion out of these refugia. This phylogeographical pattern is apparently inconsistent with the prediction based on palaeo-biome that temperate evergreen forests in subtropical mainland China migrated to the tropical south ($\leq 24°$ N) without leaving forest stands in the north during the LGM, and recolonized their present-day range from the south post-glacially (Yu *et al.*, 2000). However, it reconciles well with the extreme physiographical heterogeneity and mild climate changes in subtropical mainland China, where no ice-sheet developed during the late Quaternary glaciations, except for some high mountains in Southwest China (Shi *et al.*, 1986).

As reported in our previous study of *T. dumosa*, both cytoplasmic and nuclear DNA markers revealed extreme genetic depauperation in the Himalayas and richness in the Hengduan Mountains populations. These patterns, together

with fossil evidence, indicate that *T. dumosa* probably recolonized the Himalayas from the Hengduan Mountains in the late Quaternary (Cun & Wang, 2010), although bottleneck can not be completely ruled out. Similar recolonization was also reported in *Taxus wallichiana* (Poudel *et al.*, 2012; Liu *et al.*, 2013); however, the timing of recolonization remains uncertain. Therefore, genetic patterns of the three hemlock species suggest that hemlock populations in the Himalayas could have experienced extinction, but most populations in other areas of subtropical mainland China possibly survived *in situ* during the late Quaternary glacial cycles.

ACKNOWLEDGEMENTS

The authors thank the anonymous referees for their insightful comments and suggestions and Mare Nazaire of the Rancho Santa Ana Botanic Garden for her careful reading of the manuscript. We also thank Jianquan Liu (Sichuan University), Cheng-Xin Fu (Zhejiang University) and Mare Nazaire for their kind help in collecting the samples of several outgroups; Xiao-Hua Jin of our institute for collecting *Tsuga chinensis*-Taiwan; Jian-Ke Yang and Lei Yu of Anhui Normal University for their assistance in the field collection; and Wan-Qing Jin for her help in DNA sequencing. This study was supported by the National Natural Science Foundation of China (grant nos 30730010, 31160047), the Key Research Program of the Chinese Academy of Sciences (KJZD-EW-L07), and Dali University (grant no. KY1019208208410).

REFERENCES

Birky, C.W., Maruyama, T. & Fuerst, P. (1983) An approach to population and evolutionary genetic theory for genes in mitochondria and chloroplasts, and some results. *Genetics*, **103**, 513–527.

Clement, M.D., Posada, D. & Crandall, K. (2000) TCS: a computer program to estimate gene genealogies. *Molecular Ecology*, **9**, 1657–1660.

Crandall, K.A. & Templeton, A.R. (1993) Empirical tests of some predictions from coalescent theory with applications to intraspecific phylogeny reconstruction. *Genetics*, **134**, 959–969.

Cun, Y.Z. & Wang, X.Q. (2010) Plant recolonization in the Himalaya from the southeastern Qinghai-Tibetan Plateau: geographical isolation contributed to high population differentiation. *Molecular Phylogenetics and Evolution*, **56**, 972–982.

Currat, M., Ruedi, M., Petit, R.J. & Excoffier, L. (2008) The hidden side of invasions: massive introgression by local genes. *Evolution*, **62**, 1908–1920.

Du, F.K., Petit, R.J. & Liu, J.Q. (2009) More introgression with less gene flow: chloroplast vs. mitochondrial DNA in the *Picea asperata* complex in China, and comparison with other conifers. *Molecular Ecology*, **18**, 1396–1407.

Du, F.K., Peng, X.L., Liu, J.Q., Lascoux, M., Hu, F.S. & Petit, R.J. (2011) Direction and extent of organelle DNA introgression between two spruce species in the Qinghai-Tibetan Plateau. *New Phytologist*, **192**, 1024–1033.

Dupanloup, I., Schneider, S. & Excoffier, L. (2002) A simulated annealing approach to define the genetic structure of populations. *Molecular Ecology*, **11**, 2571–2581.

Excoffier, L., Smouse, P.E. & Quattro, J.M. (1992) Analysis of molecular variance inferred from metric distances among DNA haplotypes: application to human mitochondrial DNA restriction data. *Genetics*, **191**, 479–491.

Excoffier, L., Laval, G. & Schneider, S. (2005) Arlequin version 3.0: an integrated software package for population genetics data analysis. *Evolutionary Bioinformatics Online*, **1**, 47–50.

Fu, Y.X. (1997) Statistical tests of neutrality of mutations against population growth, hitchhiking and background selection. *Genetics*, **147**, 915–925.

Fu, L.G., Li, N. & Mill, R.R. (1999) *Tsuga. Flora of China*, Vol. 4 (ed. by Z.Y. Wu and P.H. Raven), pp. 39–41. Science Press, Beijing and Missouri Botanical Garden Press, St Louis, MO.

Gömöry, D., Paule, L., Krajmerová, D., Romšáková, I. & Longauer, R. (2012) Admixture of genetic lineages of different glacial origin: a case study of *Abies alba* Mill. in the Carpathians. *Plant Systematics and Evolution*, **298**, 703–712.

Gong, W., Chen, C., Dobeš, C., Fu, C.X. & Koch, M.A. (2008) Phylogeography of a living fossil: Pleistocene glaciations forced *Ginkgo bioloba* L. (Ginkgoaceae) into two refuge areas in China with limited subsequent postglacial expansion. *Molecular Phylogenetics and Evolution*, **48**, 1094–1105.

Gottlieb, L.D., Warwick, S.I. & Ford, V.S. (1985) Morphological and electrophoretic divergence between *Layia discoidea* and *L. glandulosa*. *Systematic Botany*, **10**, 484–495.

Hasegawa, M., Kishino, H. & Yano, T.A. (1985) Dating of the human-ape splitting by a molecular clock of mitochondrial DNA. *Journal of Molecular Evolution*, **22**, 160–174.

Havill, N.P., Campbell, C.S., Vining, T.F., LePage, B., Bayer, R. & Donoghue, M.J. (2008) Phylogeny and biogeography of *Tsuga* (Pinaceae) inferred from nuclear ribosomal ITS and chloroplast DNA sequence data. *Systematic Botany*, **33**, 478–489.

Hey, J. (2010) The divergence of chimpanzee species and subspecies as revealed in multipopulation isolation-with-migration analyses. *Molecular Biology and Evolution*, **27**, 921–933.

Hey, J. & Nielsen, R. (2007) Integration within the Felsenstein equation for improved Markov chain Monte Carlo methods in population genetics. *Proceedings of the National Academy of Sciences USA*, **104**, 2785–2790.

Hoelzer, G.A. (1997) Inferring phylogenies from mtDNA variation: mitochondrial-gene trees versus nuclear-gene trees revisited. *Evolution*, **51**, 622–626.

Jaramillo-Correa, J.P. & Bousquet, J. (2003) New evidence from mitochondrial DNA of a progenitor-derivative species relationship between black spruce and red spruce (Pinaceae). *American Journal of Botany*, **90**, 1801–1806.

Jaramillo-Correa, J.P., Aguirre-Planter, E., Khasa, D.P., Eguiarte, L.E., Piñero, D., Furnier, G.R. & Bousquet, J. (2008) Ancestry and divergence of subtropical montane forest isolates: molecular biogeography the genus *Abies* (Pinaceae) in southern Mexico and Guatemala. *Molecular Ecology*, **17**, 2476–2490.

Klymiuk, A.A. & Stockey, R.A. (2012) A Lower Cretaceous (Valanginian) seed cone provides the earliest fossil record for *Picea* (Pinaceae). *American Journal of Botany*, **99**, 1069–1082.

Li, Y., Yan, H.F. & Ge, X.J. (2012) Phylogeographic analysis and environmental niche modeling of widespread shrub *Rhododendron simsii* in China reveals multiple glacial refugia during the last glacial maximum. *Journal of Systematics and Evolution*, **50**, 362–373.

Liepelt, S., Cheddadi, R., de Beaulieu, J.L., Fady, B., Gömöry, D., Hussendörfer, E., Konnert, M., Litt, T., Longauer, R., Terhurne-Berson, R. & Ziegenhagen, B. (2009) Postglacial range expansion and its genetic imprints in *Abies alba* (Mill.) – a synthesis from palaeobotanic and genetic data. *Review of Palaeobotany and Palynology*, **153**, 139–149.

Liu, J., Möller, M., Provan, J., Gao, L.M., Poudel, R.M. & Li, D.Z. (2013) Geological and ecological factors drive cryptic speciation of yews in a biodiversity hotspot. *New Phytologist*, **199**, 1093–1108.

Matos, J.A. & Schaal, B.A. (2000) Chloroplast evolution in the *Pinus montezumae* complex: a coalescent approach to hybridization. *Evolution*, **54**, 1218–1233.

Mogensen, H.L. (1996) The hows and ways of cytoplasmic inheritance in seed plants. *American Journal of Botany*, **83**, 383–404.

Nei, M. & Takahata, N. (1993) Effective population size, genetic diversity, and coalescence time in subdivided populations. *Journal of Molecular Evolution*, **37**, 240–244.

Nielsen, R. & Wakeley, J. (2001) Distinguishing migration from isolation: a Markov chain Monte Carlo approach. *Genetics*, **158**, 885–896.

Palme, A.E., Su, Q., Palsson, S. & Lascoux, M. (2004) Extensive sharing of chloroplast haplotypes among European birches indicates hybridization among *Betula pendula*, *B. pubescens* and *B. nana*. *Molecular Ecology*, **13**, 167–178.

Perron, M., Perry, D.J., Andalo, C. & Bousquet, J. (2000) Evidence from sequence-tagged-site markers of a recent progenitor-derivative species pair in conifers. *Proceedings of the National Academy of Sciences USA*, **97**, 11331–11336.

Petit, R.J. & Excoffier, L. (2009) Gene flow and species delimitation. *Trends in Ecology and Evolution*, **24**, 383–393.

Petit, R.J., Duminil, J., Fineschi, S., Fineschi, S., Hampe, A., Salvini, D. & Vendramin, G.G. (2005) Comparative organization of chloroplast, mitochondrial and nuclear diversity in plant populations. *Molecular Ecology*, **14**, 689–701.

Pons, O. & Petit, R.J. (1996) Measuring and testing genetic differentiation with ordered versus unordered alleles. *Genetics*, **144**, 1237–1245.

Poudel, R.C., Möller, M., Gao, L.M., Ahrends, A., Baral, S.R., Liu, J., Thomas, P. & Li, D.Z. (2012) Using morphological, molecular and climatic data to delimitate yews along the Hindu Kush-Himalaya and adjacent regions. *PLoS ONE*, **7**, e46873.

Qiu, Y.X., Fu, C.X. & Comes, H.P. (2011) Plant molecular phylogeography in China and adjacent regions: tracing the genetic imprints of Quaternary climate and environmental change in the world's most diverse temperate flora. *Molecular Phylogenetics and Evolution*, **59**, 225–244.

Ran, J.H., Wei, X.X. & Wang, X.Q. (2006) Molecular phylogeny and biogeography of *Picea* (Pinaceae): implications for phylogeographical studies using cytoplasmic haplotypes. *Molecular Phylogenetics and Evolution*, **41**, 405–419.

Rieseberg, L.H. & Brouillet, L. (1994) Are many plant species paraphyletic? *Taxon*, **43**, 21–32.

Shi, Y.F., Ren, B.G., Wang, J.T. & Derbyshire, E. (1986) Quaternary glaciation in China. *Quaternary Science Reviews*, **5**, 503–507.

Shi, Y.F., Li, J.J. & Li, B.Y. (1998) *Uplift and environmental changes of Qinghai-Tibetan Plateau in the late Cenozoic*. Guangdong Science & Technology Press, Guangzhou, China.

Strasburg, J.L. & Rieseberg, L.H. (2010) How robust are "isolation with migration" analyses to violations of the IM model? A simulation study. *Molecular Biology and Evolution*, **27**, 297–310.

Wakeley, J. (2000) The effects of subdivision on the genetic divergence of population and species. *Evolution*, **54**, 1092–1101.

Wang, X.Q., Tank, D.C. & Sang, T. (2000) Phylogeny and divergence times in Pinaceae: evidence from three genomes. *Molecular Biology and Evolution*, **17**, 773–781.

Willyard, A., Cronn, R. & Liston, A. (2009) Reticulate evolution and incomplete lineage sorting among the ponderosa pines. *Molecular Phylogenetics and Evolution*, **52**, 498–511.

Yie, D.Z. & Gao, Y.X. (1979) *The meteorology of the Qinghai-Xizang Plateau*. Meteorology Press, Beijing.

Yu, G., Chen, X., Ni, J. *et al.* (2000) Palaeovegetation of China: a pollen data-based on synthesis for the mid-Holocene and last glacial maximum. *Journal of Biogeography*, **27**, 635–664.

Zhang, X.M., Gao, L.M., Möller, M. & Li, D.Z. (2009) Molecular evidence for fragmentation among populations of *Taxus wallichiana* var. *mairei*, a highly endangered conifer in China. *Canadian Journal of Forest Research*, **39**, 755–764.

Zheng, W.J. & Fu, L.G. (1978) *Tsuga*. *Flora Reipublicae Popularis Sinicae*, Vol. 7 (ed. by Delectis Florae Reipublicae Popularis Sinicae, Agendae Academiae Sinicae Edita), pp. 106–120. Science Press, Beijing.

Zhou, Y.F., Abbott, R.J., Jiang, Z.Y., Du, F.K., Milne, R.I. & Liu, J.Q. (2010) Gene flow and species delimitation: a case study of two pine species with overlapping distributions in southeast China. *Evolution*, **64**, 2342–2352.

SUPPORTING INFORMATION

Additional Supporting Information may be found in the online version of this article:

Appendix S1 Population sampling and DNA markers used in the present study.

Appendix S2 Phylogenetic reconstruction and divergence time estimation for *Tsuga* species.

Appendix S3 Counts of chlorotypes and mitotypes in populations of the three hemlock species.

BIOSKETCHES

Yu-Zhi Cun has a PhD in biology under the supervision of X.Q.W. His research interests include the evolutionary process underlying the population differentiation of conifers from subtropical mainland Asia and plant speciation in the Qinghai-Tibetan Plateau. He is now located at Dali University, and works on the phylogeography and speciation of hemlocks from East Asia.

Xiao-Quan Wang is director of the State Key Laboratory of Systematic and Evolutionary Botany, Institute of Botany, Chinese Academy of Sciences. He works on the phylogeny, evolution and biogeography of gymnosperms and orchids, and the phylogeography and speciation of plants in the Qinghai-Tibetan Plateau. He is also involved in the study of gene family evolution.

Editor: Hans-Peter Comes